Robotica (2003) volume 21, pp. 453–460. © 2003 Cambridge University Press
DOI: 10.1017/S0263574702004666 Printed in the United Kingdom

The bristle theory and traction experiment of a brush based rescue robot

Zhelong Wang and Ernest Appleton

School of Engineering, University of Durham, Durham, DH1 3LE (U.K.)
zhelong.wang@durham.ac.uk

(Received in Final Form: October 20, 2002)

SUMMARY
This work introduces the concept of a brush-based tractor used for rescue in collapsed buildings or tunnels. The paper presents the bristle theory and traction experiments relating to a robot, which uses a sensor system for detecting the shapes of pipes or tunnel like voids within rubble. Traction experiments in the laboratory were used to investigate the characteristics of bristles and the performance of the brush units of different shapes. The experimental results are discussed in the paper and related to a single bristle theory with a view to giving guidance for the design of a future brush based rescue robot in debris.

KEYWORDS: Bristle theory; Robot traction; Brush based traction; Rescue robot; Shape change.

1. INTRODUCTION

A brush based pipeline tractor has been proposed and developed by the Centre for Industrial Automation and Manufacturing (CIAM), School of Engineering, University of Durham.[1,2] The university holds a number of worldwide patents relating to such devices. Movement of the tractor is achieved by the utilisation of curved bristles as a means of propulsion and support, as illustrated in Figure 1. If the cylinder opens, the leading brush, offering lower resistance because of the bristle curvature, moves forward easily. The trailing brush, because of its higher resistance to backward forces, remains stationary, effectively gripping the pipe wall. However, when the reverse happens, that is, the cylinder closes, the leading brush remains stationary, whereas the trailing brush, now encountering lower reverse resistance, is pulled forward.

Based on this principle, a brush based rescue robot has been proposed. It has been developed to be able to change its body shape to allow it to fit voids or pipes with varied cross sections. Figure 2 shows the structure of the robot body module. In the design concept the bristles are mounted on a flexible steel hoop held in position by four stepper motor driven actuators. A useful measure of traction efficiency is the ratio of forward force to reversal force. If the actuator moves, the spring steel hoop can change its shape to form an ellipse, rectangle, square or diamond. Thus, the robot body can be made to fit the void as closely as possible and the bristles contacting the void wall can be bent to an optimum shape to achieve the best traction performance. Thus it is necessary to understand the characteristics and behaviour of individual bristles. And it is also important to know which shape of the robot body will achieve the best traction.

2. TRACTION EXPERIMENTS

One aim of this research was to understand how brush units of different shapes could achieve the optimum traction force

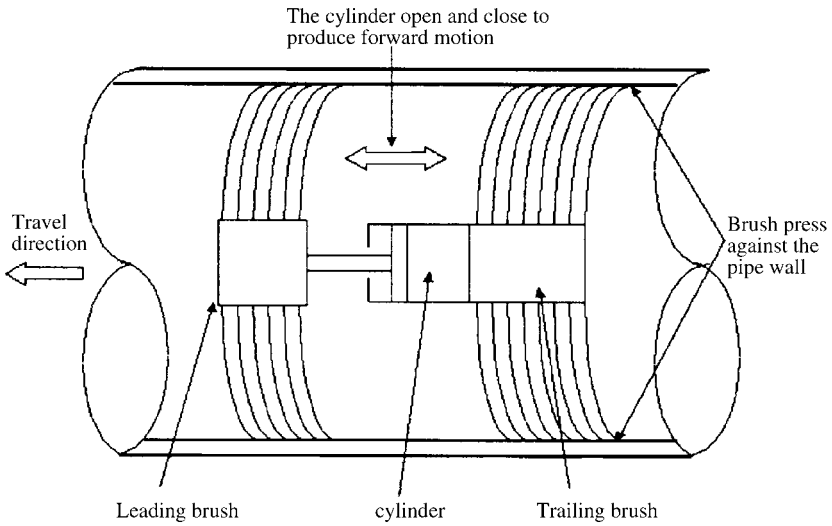

Fig. 1. The working mechanism of a brush robot.

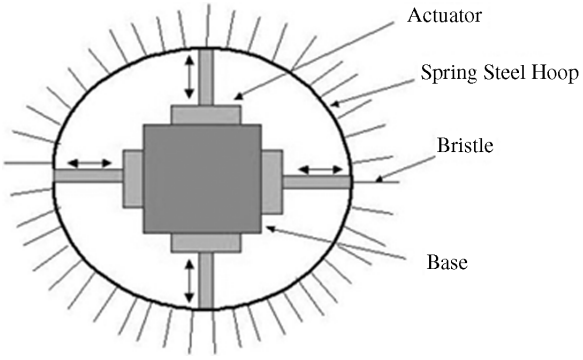

Fig. 2. The structure of one robot body module.

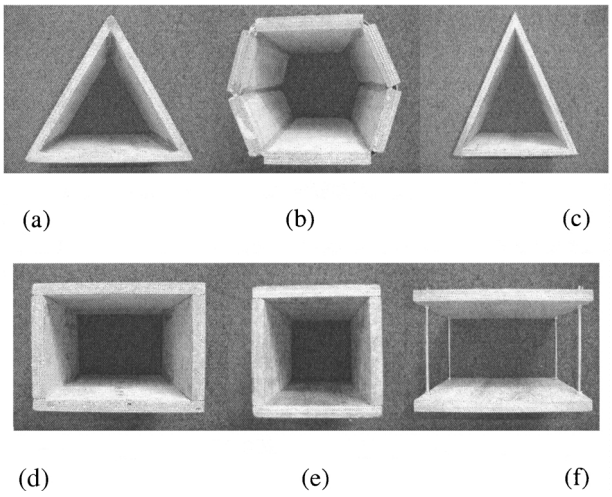

Fig. 3. Boxes of different geometry shapes.

in different voids. Two forces are important in this form of traction: the force needed to push a brush forward along the pipe, and the reversal force on the gripping until it collapses or slides backwards. Traction force experiments were carried in the laboratory in which brush units of different geometric shapes were used to simulate the robot body modules of different shapes. Several wooden boxes of different shapes were used to simulate voids of various shapes. In a real environment, the void shape will be more complicated than the simple geometric shapes investigated here but this simulation of the problem was considered approximate at this initial stage of the research. The boxes used in the experiment are shown in Figure 3. Brush units used in the tests had the shapes shown in Figure 4, including (a) circle, (b) ellipse, (c) rectangle, (d) approximate square and square. These brush units have geometrical shapes corresponding to the potential robot body module shapes achievable by deflecting the flexible steel hoop. All brush units were populated with a similar amount of bristles; all brush units have bristles arranged in 8 rows, 32 holes per circumference, giving a total of 256 holes for each brush unit.

2.1. Introduction to traction test equiment and procedure

Figure 5 shows the rig layout. A "Clockhouse" compression-testing machine was used as the "platform" for these tests. As the traction tests involved brush units being

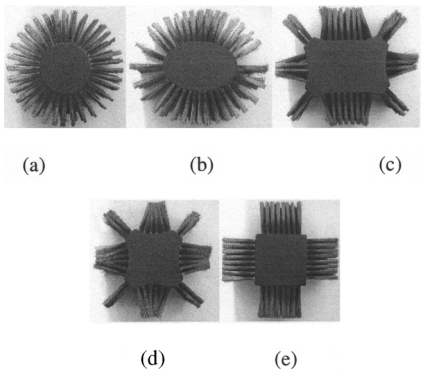

Fig. 4. Brush units in different geometry shapes.

"pushed" through the void boxes, a compression-testing machine provided an ideal platform on which tests to conduct tests. All tests were carried out with the compression-testing machine operating at its fastest speed of 0.174 mm/s. However, it should be noted that this may be a lower speed than that for a brush unit whilst deployed in a real application. Additionally, a robot operating within a pipeline or a void applies the axial thrust or pull to its brushes in a rapid cycle. Thus, in practice, a brush unit would experience rapid acceleration and deceleration, which is not the case in these tests. The dynamic performance of brush units is a subject for further investigation.

During their manufacture, the boxes shown in Figure 3 were placed in a lathe and both ends were faced off. This ensured that the axis of the box maintained perpendicular to the loading platform of the testing machine.

In Figure 6, the "Clockhouse" testing machine consisted of a machined loading plate, which was located on the top of the lifting platform of the machine. A linear transducer was connected to a displacement shaft contacting the lifting platform. After calibration, the linear transducer provided an accurate measurement of the distance travelled. To ensure that the brush unit remained as central as possible within the

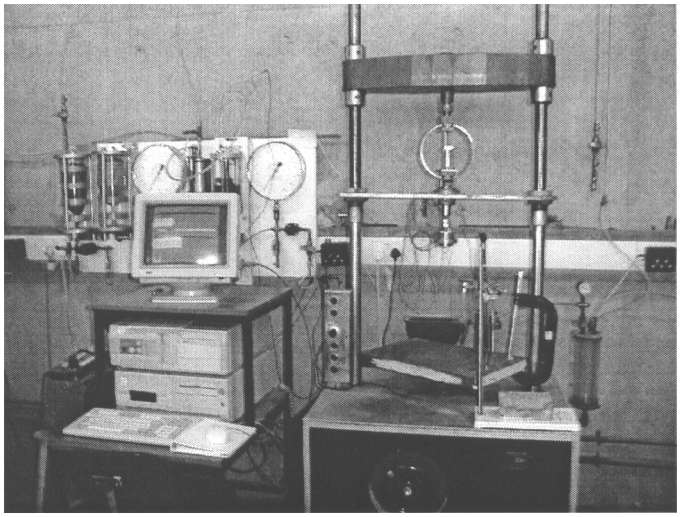

Fig. 5. A "Clockhouse" compression-testing machine.

https://doi.org/10.1017/S0263574703004661 Published online by Cambridge University Press

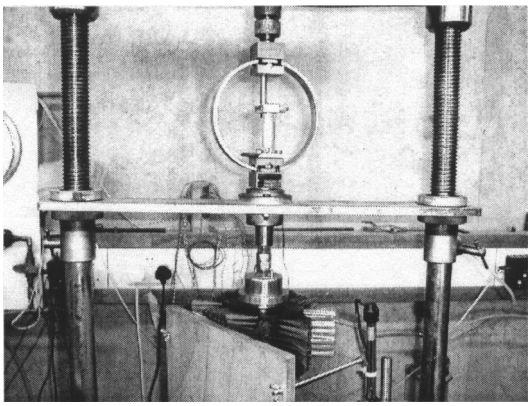

Fig. 6. Experiment set up.

box, a push plate with two pins was used (Figure 6). The push plate was placed against the brush unit and two pins on the push plate thrust into two holes in the brush unit, which stops the rotation of the brush unit. The distance between the two holes is the same as the distance between the two pins on the push plate and the holes are symmetrical about the central axis of the brush core. The two pins are also symmetrical about the central axis of push plate. The push plate was attached to a steel shaft, which ran inside an axial bearing housing on the compression-testing machine. The bearing housing ensured that the push plate pushed the brush unit as centrally as possible. The bearing housing was integrated into the cross-brace support of the compression-testing machine. This assembly was further connected to a "proving" ring. Prior to beginning the experiments, both the proving ring and displacement transducer were calibrated. The two rings used for testing were a 200 Kg (force, 1960 N) ring (No. 2667-transducer: 0.04645 kg/mv) and a 1000 Kg (force, 980 N) ring (No. 2380-transducer: 0.2209 kg/mv). A personal computer was connected to the linear displacement transducer and the proving ring via cables. The software package TRIAX, running on the PC, collected and recorded signals from the transducers.[3]

The operation of the experiment involved the following steps:

After the brush unit had been located into position, the machine was switched on. The lifting platform was then raised; this subsequently raised the box, which was located on a rectangular plate. As the brush unit touched the top of the box, the brush unit bristles began to sweep back and the top of the proving ring contacted the large cast iron reaction support. This was the point at which the brush began to be inserted into the box. As the test continued and the brush unit became fully inserted into the box, the force required to push the brush unit forward and the travelled displacement of the brush unit were recorded. The support plate of the compression-testing machine was then lowered and the box was inverted, while the brush unit remained inside. The above experiment was then repeated; however, this time, the brush unit was forced to reverse. Once again, the transducer and proving ring signals were collected and recorded by using the software TRIAX. Subsequently, the force exerted was plotted against the vertical displacement of the brush unit.

2.2. Brush unit forward traction tests

Each brush unit was tested in different boxes to investigate in which box the brush unit could achieve the biggest traction force. So, the following test combinations were investigated for this purpose:

- An elliptical brush unit, a square brush unit, a circular brush unit, a rectangular brush unit and an approximate square unit were tested separately between two parallel boards.
- An elliptical brush unit, a square brush unit, a circular brush unit, a rectangular brush unit and an approximate square unit were tested separately in a rectangular box.
- An elliptical brush unit was tested in a hexagonal box.
- An elliptical brush unit, a rectangular brush and an approximate square unit were tested separately in an isosceles triangle box.
- A square brush unit, an approximate square unit and a circular brush were tested separately in a square box
- A circular brush unit and an approximate square unit were tested separately in an equilateral triangle box.

All test results were recorded and plotted giving traction force against brush unit vertical displacement, as shown in Figure 7. Each test was repeated three times and the software package ORIGIN plotted the average value curve of the three repeated tests.[4] For clarity, only the average curve is shown in the graphs.

2.3. Brush unit reverse traction tests

Similar to the tests described in the paragraph above, all brush units were also subjected to a reverse traction test. Due to the large forces involved in the reverse traction test, a 1000 Kg proving ring (No. 2380-transducer: 0.2209 kg/mv) was chosen for the reverse test. The test procedure was the same as the forward traction test; all signals from the linear displacement transducer and the proving ring were recorded and then plotted as traction force against the brush unit vertical displacement (Figure 8).

For both forward traction and reverse traction, every test was repeated three times and the software package ORIGIN plotted the result of each test. Then, the software did a curve fitting operation to each plot and plotted an average curve. For clarity, only the average curve is shown in the graphs.

In this description comparisons are made between the performances of different shaped brushes in different shaped boxes. In the discussion reference is made to particular comparison using brushes that are subjectively but obviously of insert. That is, a comparison is made of brush units tested in boxes, which have a reasonably similar shape to the brush unit or have reasonable contacting surface with the brush unit. For example, a circular brush, a square brush and an approximate square brush can be tested in a square box; but it is obviously not reasonable to test an elliptical brush in a square box.

2.4. Discussions of the traction experimental results

The experimental results in Figure 7 and Figure 8 show that a brush unit needs to have the similar shape to the box and the biggest contacting surface with the box. For example, a

https://doi.org/10.1017/S0263574703004661 Published online by Cambridge University Press

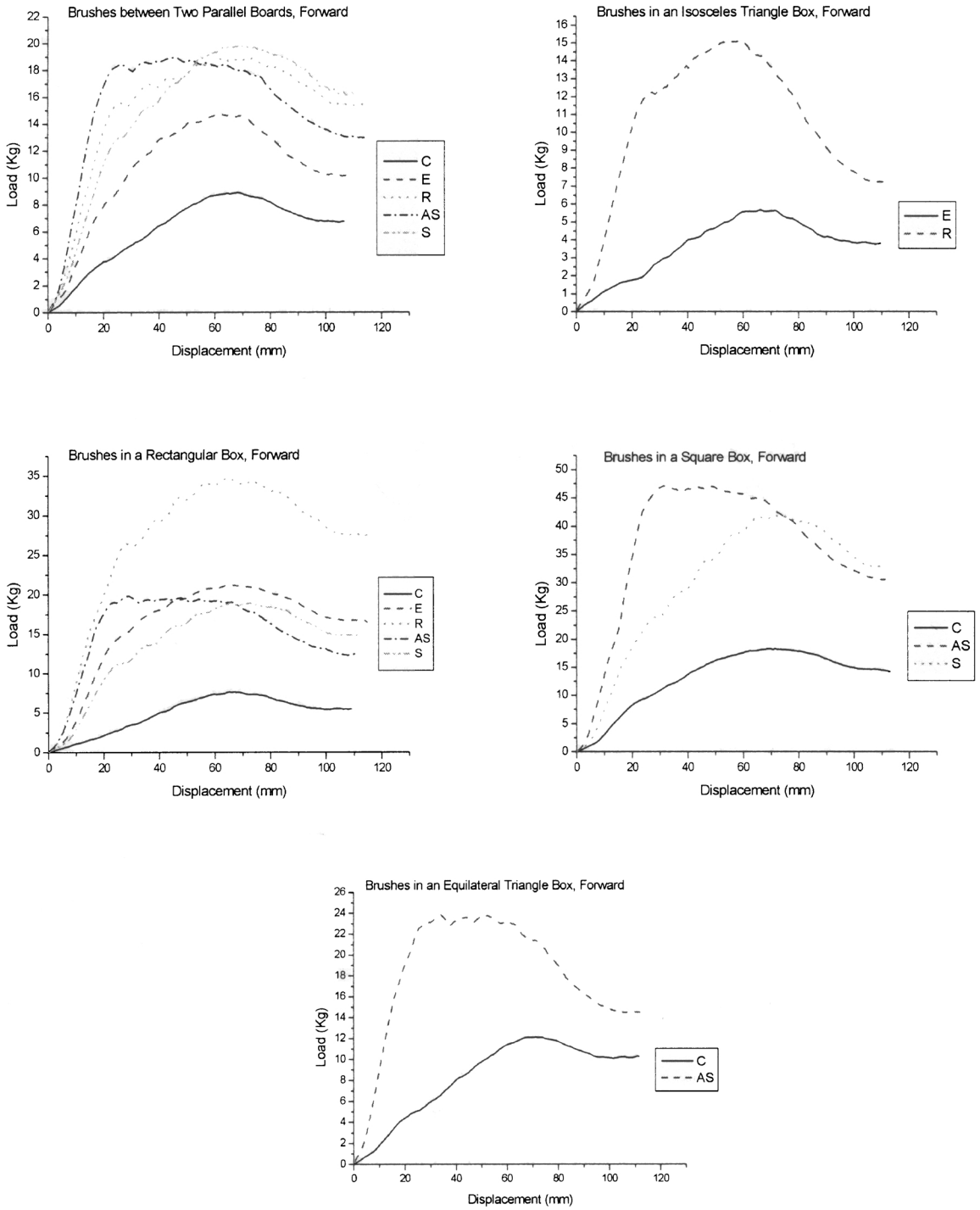

Fig. 7. Brush units forward traction experiments (*Note*: C: circle, E: ellipse, R: rectangle, AS: approximate square, S: square).

rectangular brush unit could achieve the biggest traction force in a rectangular box for both forward traction test and reverse test. An approximate square brush unit could achieve the biggest traction force in a square box for both forward traction test and reverse test. It was noticed that an approximate square brush unit could achieve a bigger traction force than a square brush unit. This is because the bristles of the approximate brush unit form a "X-ply" mechanism and this can help to increase traction force remarkably. More details about "X-ply" mechanism can be found in reference [1].

Figure 9 shows the force diagram of one bristle when a brush unit is doing a reverse traction test. One end of the bristle is fixed on the brush unit core and the other end of the bristle contacts the surface of the pipe wall. A bristle can be considered as a strut, that is, a compression member, which is long compared to its cross-sectional area. The buckling theory suggests that such a member will fail due to buckling before the direct compressive stress reaches the yield point. Euler theory considers the axial load required to buckle a strut but the limitation to apply Euler is that the strut needs to be initially straight. Additionally, the load

https://doi.org/10.1017/S0263574703004661 Published online by Cambridge University Press

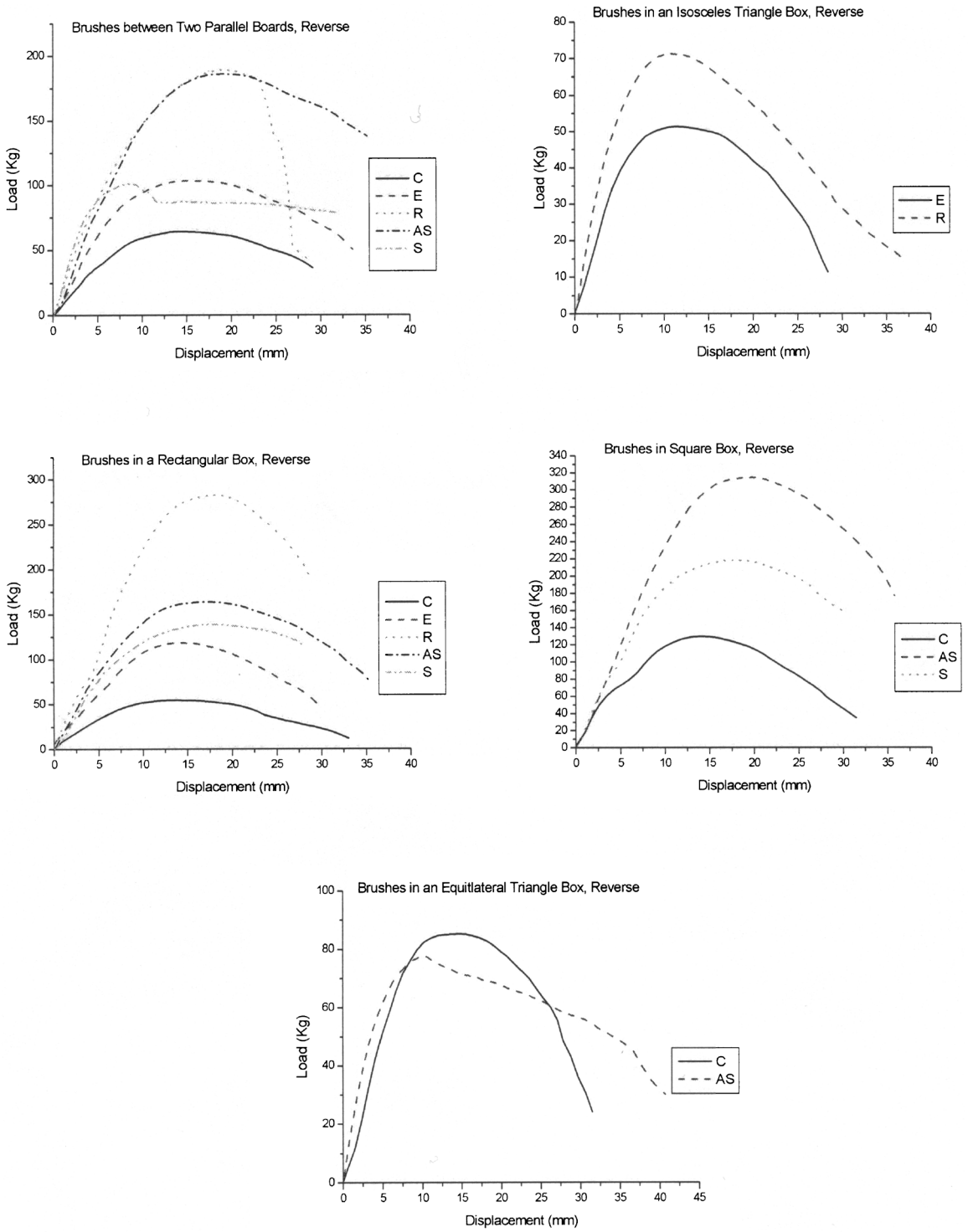

Fig. 8. Brush units reverse traction experiments (Note: C: circle, E: ellipse, R: rectangle, AS: approximate square, S: square).

must be applied axially and the material must be homogenous. However, the buckling theory does provide a useful insight into how a bristle behaves under different constraint conditions. The Euler theory includes four different constraint cases:[5]

(i) Strut with both ends pinned,
(ii) Strut with one end fixed and one end free,
(iii) Strut with both ends fixed,
(iv) Strut with one end fixed and one end pinned.

When a bristled brush is inserted into a pipe and subjected to a reversal force, the brush would normally reverse by core rotation as if it were in reverse or gripping mode. That is, the bristles move out of plane and a couple is induced into the brush core. Equation (1) illustrates the different modes of the Euler theory model applicable to the brush mechanism.

In the reverse traction experiments, the brush units have two tendencies dependent on the experimental conditions. One tendency is that the brush unit rotates in the perpendicular plane to the brush axis. This happens to circular brush units and elliptical brush units. The Euler theory model is applicable to this case; that is mode (ii) "Strut with one end fixed and one end free" and for this

https://doi.org/10.1017/S0263574703004661 Published online by Cambridge University Press

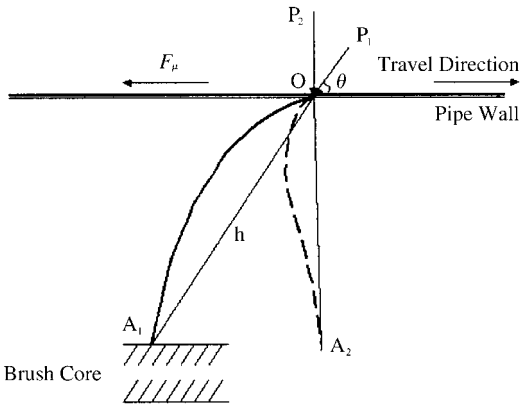

Fig. 9. The diagram of one bristle acting on the pipe wall.

mode $K=0.25$. The other tendency is that the brush unit buckles in the transverse plane to the brush axis and flips out of the perpendicular plane to the brush axis. This happens to rectangular and square brushes. The Euler theory model is applicable to these cases; that is mode (iv) "Strut with one end fixed and one end pinned" and for this mode $K=2.05$. Comparing these two different modes, it can be seen that a higher reversal load is obtained when the brush unit is not allowed to rotate in the box.

In Figure 9, the bristle moves towards the right. h is the distance between point O and the bristle end on the brush core. Here, the bristle is assumed relatively straight so h is further approximately assumed as the length of the bristle. As the brush core moves, the bristle end on the brush core moves from A_1 to A_2. P is the thrust force along the bristle axial direction OA_1. Based on the assumptions above and Euler theory, P can be expressed by the following equation:[5]

$$P=\frac{K\pi^2 EI}{h^2} \tag{1}$$

In the experiment, the travel speed of the brush unit was low. So, the bristles of the brush unit experienced the following process. Reference to the stage OA in Figure 10, shows that the bristle has no sign of slipping and is in the gripping mode when the reverse traction test starts. The traction force increases sharply. Stage AB shows that the bristle starts to deflect and is unable to take the load.

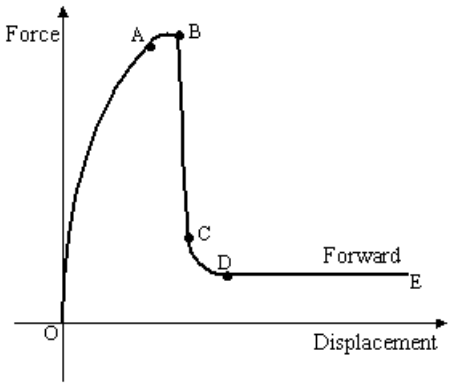

Fig. 10. The traction force change in the reverse traction experiment.

At the point B, the bristle collapses rapidly due to buckling failure, which is an instability condition. Stage BC shows that the bristle flips out of the plane and the traction force decrease sharply. The steepness of the curve in this stage is dependent upon test conditions. The gradient of the curve has little meaning because it follows an instability condition and is test dependent. Stage CD of the curve shows how displacement begins to take place in a steady manner and the gradually decreased force that will move the brush down in a "forward traction" process. Stage DE shows that bristle in a forward traction status and the traction force has a stable value.

3. BRISTLE THEORY FOR THE BRUSH ROBOT

3.1. Bristle forward theory

Stutchbury[1] did some work in bristle theory in his thesis. He considered a bristle sliding forwards through pipe as shown in Figure 11. It can be assumed that the bristle forms an angle with the pipe wall; this is represented by the line OH. If the bristle is moved towards the left, its motion will be opposed by a friction force μF, where F is the force normal to the pipe wall caused by the bristle resilience. A brush inside a pipe will be in transverse equilibrium so that the sum of all the F values for all the bristles extending from the brush core will be zero and the sum of all the μF components will equal the total force required to move the brush through the pipe in a forward direction. The sum of the force vectors (F) perpendicular to the pipe wall and the frictional force μF is the resultant force OC. Note that in the limiting case, the angle between OA and OC is the friction angle θ such that $tg\,\theta=\mu$. The resultant force OC can be resolved into two components, one perpendicular to the bristle OD and one component along the bristle DC. If the bristle is relatively straight and the thrust along the bristle is not sufficient to cause buckling, the bending of the bristle can be assumed to be caused by the bending force OD acting perpendicular to the bristle.

3.2. Bristle reverse theory

If the brush is then put into gripping mode by pushing the core in the opposite direction, the frictional force direction will be reversed. Assuming that the value of μ is the same in both directions, then the resultant force acting on the bristle tip will be along the line OE where the angle between OE and the pipe wall is once again θ, the friction angle. Although the limiting line of action of the resultant force acting on the bristle in gripping mode is known at this stage, the magnitude of the resultant force has yet to be determined. In a forward sliding mode it was assumed that the shape of the bristle, that is the bending of the bristle, was determined by the bending force OD. If it is further assumed that the shape of the bristle remains the same in gripping mode, only the thrust along the bristle increases. If the line of the thrust along the bristle is extended, it will eventually intersect with the friction angle line OE giving a thrust magnitude DE. From Figure 11 it can be seen that in a gripping mode the resultant force acting at the bristle tip is OE, which can be resolved into two components, OD

https://doi.org/10.1017/S0263574703004661 Published online by Cambridge University Press

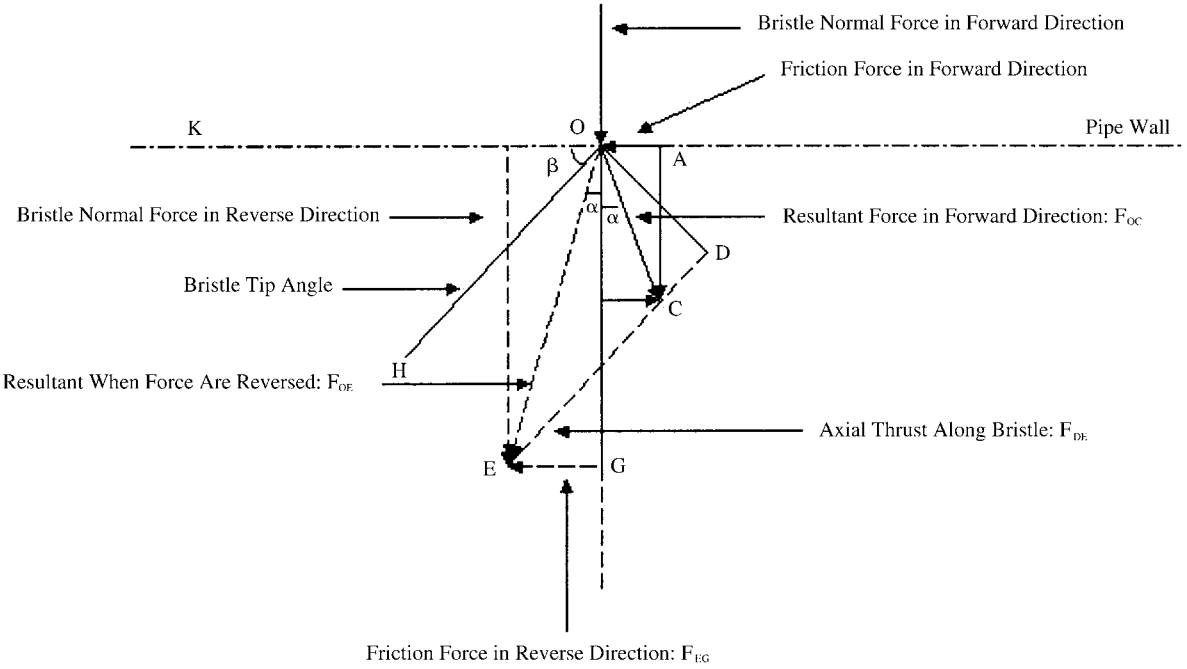

Fig. 11. Model illustrating bristle force.

perpendicular to the bristle and DE along the bristle. Resolving the resultants into the direction along the pipe axis, in both the forward slide and gripping modes, the ratio of the traction force required to push a brush forward and the limiting force available in the gripping mode can be calculated, that is GE/BC. The model developed provided a method of predicting the forward to reverse, or "slip to grip", ratio, for given frictional conditions. This model is deemed satisfactory up to the onset of bristle buckling.

3.2.1. Mathematical discussion of bristle reverse theory. In Figure 11, OH is the bristle tip and $\angle KOH=\beta$ is the bristle tip angle. $\angle KOE=\theta$ is the friction angle of the bristle. $OH\perp OD$, μ is a friction coefficient and α is constant. It is assumed that F_{OD} remains the same in gripping mode as it does in the forward direction, so F_{OD} is constant. In the force diagram of Figure 11, the thrust along the bristle DE increases considerably if the angle β between the bristle and pipe wall approaches the friction angle θ. When the angle β is equal to the friction angle θ, the vector representing the thrust force along the bristle (extension of DC) is parallel to the vector of the resultant acting along the frictional angle line OE, i.e. a theoretical thrust along the bristle is infinite since all these lines theoretically meet at infinity. These conclusions can be explained by the following mathematical discussion. From the geometry of the Figure 11, the following equations can be acquired,

$$\angle HOE=90-\alpha-\beta, \tag{2}$$

$$\angle DOC=90-2\alpha-\angle HOE=\beta-\alpha, \tag{3}$$

$$\angle EOD=2\alpha+\angle DOC=\beta+\alpha \tag{4}$$

Thus,

$$F_{OE}=\frac{F_{OD}}{\cos\angle EOD}=\frac{F_{OD}}{\cos(\alpha+\beta)}, \tag{5}$$

$$F_{EG}=F_{OE}\sin\alpha=\frac{F_{OD}\sin\alpha}{\cos(\alpha+\beta)}, \tag{6}$$

$$\text{When } \beta\uparrow\Rightarrow\cos(\alpha+\beta)\downarrow\Rightarrow\frac{F_{OD}}{\cos(\alpha+\beta)}\uparrow\Rightarrow F_{EG}\uparrow,$$

(Note: ↑ increase, ↓ decrease, ⇒ lead to)

$$\text{When } \beta\downarrow\Rightarrow\cos(\alpha+\beta)\uparrow\Rightarrow\frac{F_{OD}}{\cos(\alpha+\beta)}\downarrow\Rightarrow F_{EG}\downarrow,$$

$$\text{When}\quad \beta=\theta\Rightarrow\alpha+\beta=90\Rightarrow\cos(\alpha+\beta)=0\Rightarrow\frac{F_{OD}}{\cos(\alpha+\beta)}$$

$=+\infty$, this explains how a theoretical thrust along the bristle is infinite when the angle β is equal to the friction angle θ. However, the bristle and the pipe wall cannot sustain thrust forces of infinity. For example, a slender bristle will collapse by elastic buckling before reaching a load of infinity. Alternatively, a short stubby bristle may collapse by plastic yielding or the failure of the pipe wall may also limit the magnitudes of the bristle thrust force. The buckling of a lender bristle is probably the mode of failure in this case and thus the magnitude of the thrust along the bristle is limited to the buckling load. Since the thrust along the bristle is limited to the buckling load, it may not be possible for the resultant force acting on the bristle tip to reach the frictional limit. Thus, in the case of a bristle failing by buckling, even if the bristle angle is near or beyond the friction angle, the

https://doi.org/10.1017/S0263574703004661 Published online by Cambridge University Press

axial force will be less than the limiting friction value and therefore the bristle will grip without slip. But, as the bristle tip rotates about O and the bristle angle moves beyond the friction angle, the axial force that the bristle can sustain decreases to zero and thus the bristle flips through, pushing the brush core along the pipe. The failure of the bristle by buckling is an instability phenomenon, so the flip through of the bristle is a quick and unstable process.

4. CONCLUSIONS

The paper focuses on the research of bristle theory for a brush based rescue robot. Through the traction experiment of the brush unit in the lab, the characteristics of the bristle and performance of the brush units of different shapes fitting in different box were investigated. Following the investigation of the traction experiment, a bristle theory for the brush based robot was modelled and could be used for guidance in the design of a future brush based rescue robot.

ACKNOWLEDGEMENT

The authors would like to express thanks to the Audi Foundation for their sponsorship to this research.

References

1. N. Stutchbury, "Design Characteristics of a Pipe Crawling Robot," **Ph.D. thesis** (University of Durham, 1999).
2. C. Han, "The Experiment Investigation of a Pipe Robot," **M.Sc. thesis** (University of Durham, 1999).
3. D. Toll, "A Computer Control System for Stress Path Triaxial Testing", *5th International Conference on Civil and Structural Engineering and Computing*, Edinburgh (1993) pp. 107–113.
4. *Getting Started Using Origin 7* (OriginLab Corporation, 2001).
5. J. Carvill, *Mechanical Engineer's Data Handbook* (Oxford: Butterworth-Heinemann, 1997).

https://doi.org/10.1017/S0263574703004661 Published online by Cambridge University Press